



Comprehensive Genomic Investigation of Tigecycline Resistance Gene *tet(X4)*-Bearing Strains Expanding among Different Settings

 Ruichao Li,^{a,b} Yan Li,^a Kai Peng,^a Yi Yin,^a  Yuan Liu,^{a,b} Tao He,^c Li Bai,^d Zhiqiang Wang^a

^aJiangsu Co-Innovation Center for Prevention and Control of Important Animal Infectious Diseases and Zoonoses, College of Veterinary Medicine, Yangzhou University, Yangzhou, People's Republic of China

^bInstitute of Comparative Medicine, Yangzhou University, Yangzhou, People's Republic of China

^cJiangsu Key Laboratory for Food Quality and Safety-State Key Laboratory Cultivation Base of Ministry of Science and Technology, Institute of Food Safety and Nutrition, Jiangsu Academy of Agricultural Sciences, Nanjing, China

^dKey Laboratory of Food Safety Risk Assessment, National Health Commission of the People's Republic of China, China National Center for Food Safety Risk Assessment, Beijing, People's Republic of China

Ruichao Li and Yan Li contributed equally to this article. Author order is determined by alphabetical order.

ABSTRACT The emergence of plasmid-mediated tigecycline resistance genes has attracted a great deal of attention globally. Currently, no comprehensive in-depth genomic epidemiology study of *tet(X4)*-bearing pathogens present of pork origin as the One Health approach has been performed. Herein, 139 fresh pork samples were collected from multiple regions in China and 58 *tet(X4)*-positive strains were identified. The *tet(X4)* gene mainly distributed in *Escherichia coli* ($n = 55$). Besides, 4 novel *tet(X4)*-positive bacterial species *Klebsiella pneumoniae* ($n = 2$), *Klebsiella quasipneumoniae* ($n = 1$), *Citrobacter braakii* ($n = 1$) and *Citrobacter freundii* ($n = 1$) were first characterized here. Four different core *tet(X4)*-bearing genetic environments and five types of *tet(X4)*-bearing tandem duplications were discovered among 58 strains. The results of the phylogenetic tree showed that there was some correlation between *E. coli* strains from pork, human, pig farms, and slaughterhouses. A total of seven types of plasmid replicons were found in *tet(X4)*-positive plasmids, among which multireplicon plasmids were observed. Notably, two *tet(X4)*-positive fusion plasmids pCSZ11R (IncX1-IncFIA-IncFIB-IncFIC) and pCSX5G-*tetX4* (IncX1-IncFII-IncFIA) were formed by IS26 in the hot spot. Besides, six samples were identified to harbor two different *tet(X4)*-bearing strains. More interestingly, the absolute quantitative results showed that the expression levels of *tet(X4)* between different strains with different *tet(X4)* copies were approximate. In this study, the genetic environment of *tet(X4)*-positive plasmids containing different plasmid replicons was analyzed to provide a basis for the further development of effective control measures. It is also highlighted that animal-borne *tet(X4)*-bearing pathogens incur a transmission risk to consumed food. Therefore, there is an urgent need for large-scale monitoring as well as the development of effective control measures.

IMPORTANCE Tigecycline was considered the last-line drug against serious infections caused by multidrug-resistant Gram-negative bacteria. However, the plasmid-mediated tigecycline resistance gene *tet(X)* has been widely reported in different sources of Enterobacterales and *Acinetobacter* in China. China is one of the largest pig-producing nations in the world, and in-depth investigation of gene in pork is vital to figure out the fundamental dissemination of these genes and set up a reasonable control framework. In this study, we conducted an in-depth and systematic analysis of the diversity of *tet(X4)*-positive plasmids and the genetic environment of *tet(X4)* contained in pork samples from multiple regions of China, providing a basis for

Editor Jasna Kovac, The Pennsylvania State University

Copyright © 2021 Li et al. This is an open-access article distributed under the terms of the [Creative Commons Attribution 4.0 International license](https://creativecommons.org/licenses/by/4.0/).

Address correspondence to Ruichao Li, rchl88@yzu.edu.cn, or Zhiqiang Wang, zqwang@yzu.edu.cn.

The authors declare no conflict of interest.

Received 20 September 2021

Accepted 17 November 2021

Published 22 December 2021

further development of effective control measures. It is also highlighted that animal-borne *tet(X4)*-bearing pathogens incur a transmission risk to consumed food. Therefore, there is an urgent need for large-scale monitoring as well as the development of effective control measures.

KEYWORDS *tet(X4)*, bacteria, plasmids, food safety, genomics, tigecycline resistance

Recently, multidrug-resistant (MDR) and extensively drug-resistant (XDR) Gram-negative pathogens pose serious threats to public health and food security (1, 2). Tigecycline was commonly used in clinical settings since it has a broad-spectrum activity (3, 4). In 2010, tigecycline was first applied in clinical treatment for treating XDR Enterobacteriaceae in China, the overexpression of efflux pumps and mutations within the tigecycline drug-binding sites were the main resistance mechanisms (5–7). However, He et al. discovered the plasmid-mediated mobile tigecycline resistance genes *tet(X3)* and *tet(X4)* in Enterobacteriaceae and *Acinetobacter* in 2019, which posed a severe threat to global public health (8). Of concern, previous studies have shown that *tet(X4)* has been found to coexist with *mcr-1* or *bla_{NDM-1}* in the same strain (9, 10). The strains resistant to multiple last-resort antibiotics regarded as new superbugs may disseminate globally.

So far, *tet(X4)* has been discovered in several bacteria species such as *Escherichia coli*, *Aeromonas caviae*, *Acinetobacter* sp., and *Escherichia fergusonii* (8, 10–12). Meanwhile, the *tet(X4)* gene is widely distributed on plasmids of diverse replicon types (13). All these results illustrated that the *tet(X4)* gene has the potential to extensively disseminate and should arouse our attention. Currently, there is no systematically investigation on the transferability and fitness of *tet(X4)*-carrying strains isolated from pork samples. Here, we analyzed the emerging *tet(X4)*-bearing strains isolated from pork samples across 10 regions of China in 2019. We found multiple distinct strains carrying the *tet(X4)* gene and illustrated the complex *tet(X4)* genetic environments, showed a possibility of *tet(X4)* spreading into the different plasmids.

RESULTS

Prevalence of *tet(X4)* positive isolates among pork in multiple regions. A total of 58 tigecycline-resistance strains were obtained from 139 samples of fresh pork. There was a difference in the positive rate of *tet(X)*-carrying bacteria among pork samples from different regions (Fig. 1). Guangdong (10/12, 83.33%), Hebei (14/19, 74.68%) and Shanxi (7/13, 53.85%) had a relatively high *tet(X)*-positive rate (Table S1). The 58 *tet(X4)*-positive strains were overwhelmingly dominated by *E. coli* (91.38%), followed by *K. pneumoniae* (3.4%), *K. quasipneumoniae* (1.7%), *Citrobacter braakii* (1.7%), and *Citrobacter freundii* (1.7%) (Table S2). To the best of our knowledge, this is the first time that *tet(X4)* has been discovered in *K. quasipneumoniae*, *C. freundii* and *C. braakii* in pork. Notably, a low number of samples and sampling bias may affect the positive rates observed.

Antimicrobial susceptibility testing, resistance genes and virulence gene. According to the result of MICs (Table S3), 58 *tet(X4)*-positive strains showed resistance to multiple drugs and were all resistant to tigecycline (8 mg/liter–64 mg/liter) and other tetracyclines (doxycycline, oxytetracycline, tetracycline, and minocycline). In addition, most of them also showed resistance to florfenicol, ceftiofur and amoxicillin. But all these strains were susceptible to meropenem and colistin. The phenotype could in most cases be explained by the carriage of the corresponding resistance genes. The *tet(X4)*-positive strains contained multiple antibiotic resistance genes (7–25), including sulfonamides (*sul* gene 45/58), aminoglycosides (*aadA*, 58/58), β -lactam (*bla_{TEM-1}* 37/58), phenicols (*floR*, 54/58), tetracyclines (*tet[A]*, 48/58), trimethoprim (*drfA12* 32/58), and quinolones (*qnrS1*, 40/58). In accordance with the findings shown in Fig. S1, most of the *E. coli* carried a little number of virulence genes. The *K. pneumoniae* SDP9R strain belonged to ST1418 and carried the yersiniabactin biosynthetic gene cluster (*ybt 10*

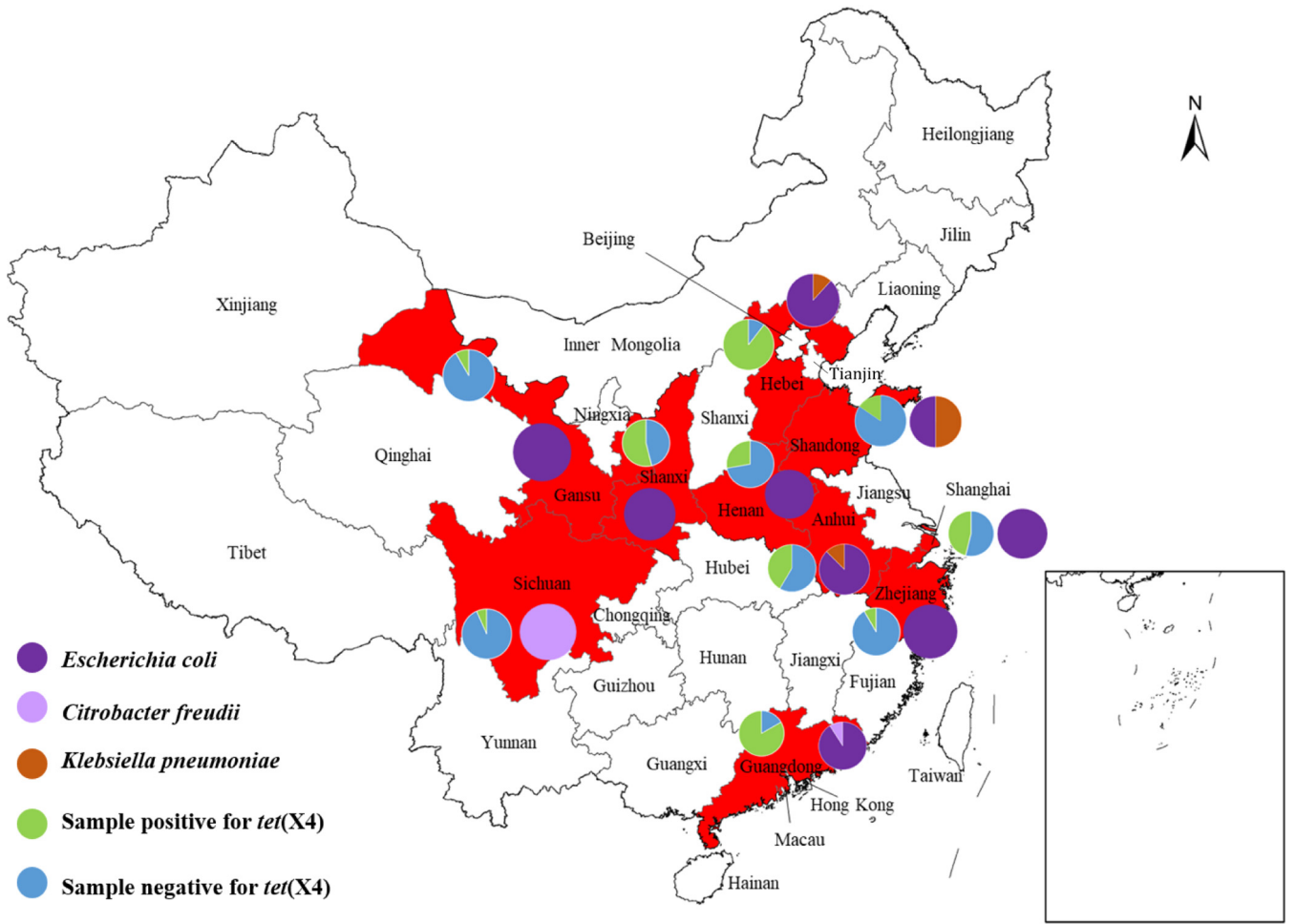


FIG 1 Map of the distribution of the collected retail pork in China. A total of 139 samples, 58 tetracycline-resistance strains. The red region represents the province in which tet(X4)-positive strains were isolated.

[YbST78] in the integrative conjugative element ICEKp4). Further, we found aerobactin (*iuc 3*, AbST23) in *K. pneumoniae* AB4-4.

A wide variety of tet(X4)-harboring plasmids. In total, the 58 tet(X4)-harboring plasmids were classified into six plasmid replicon types. As shown in Fig. 2 and Table S4, the IncX1 and IncFIA-IncHI1B-IncHI1A type plasmids were observed to be the most prevalent. The IncX1 type plasmids were detected in multiple species and

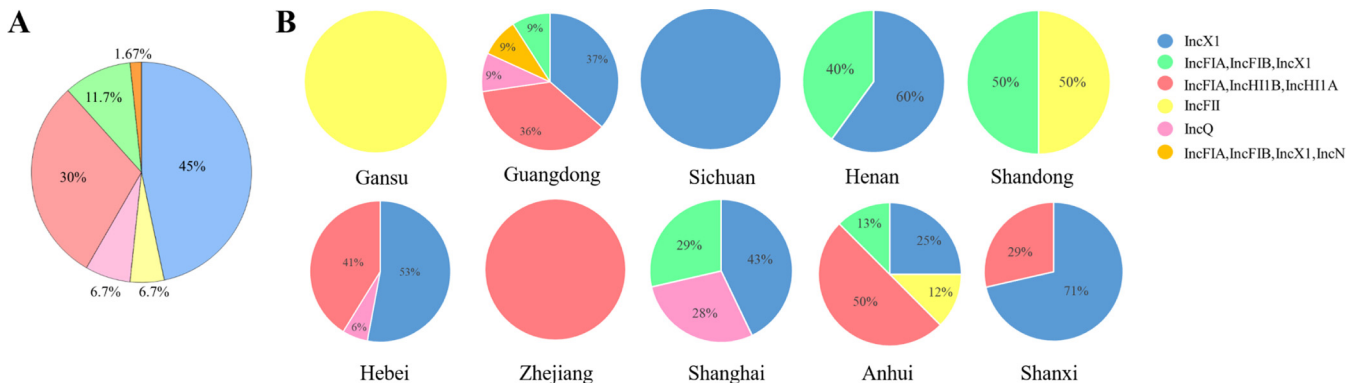


FIG 2 The distribution of different Inc group plasmids in all tet(X4)-positive strains. (A) The percentage of Inc groups found in all tet(X4)-positive strains. (B) The distribution of the different Inc groups in 10 regions.

provinces, which further illustrated the widespread dissemination of IncX1 type plasmid carrying *tet(X4)*. Besides, plasmids of 18 representative *tet(X4)*-positive strains were selected for Nanopore long-read sequencing. Sixteen circular *tet(X4)*-encoding plasmids were obtained from these isolates (Table S5); another two plasmids pHN13R-*tetX4* and pAB12-1-*tetX4* contained multiple copy numbers of the *tet(X4)*-bearing regions. As shown in Table S5, a total of six plasmid Inc types were obtained from 18 plasmids.

Among the 18 plasmids, there were eight IncX1-type plasmids with a size range of positions 31–57 kb (Fig. S2). In the NCBI database, plasmid pYY76-1-2 (CP040929) was the first discovered IncX1 type plasmid carrying the *tet(X4)* gene, which was collected from cattle feces and shared high similar backbones to IncX1 plasmids in this study. The main difference between these IncX1 type plasmids was the presence or absence of type IV secretion system (T4SS) gene cluster. The IncQ type plasmid pH52-1-*tetX4* and pSH12R-*tetX4* showed high plasmid-backbone similarities (BLASTN) with that of *tet(X4)*-positive plasmid pLHM10-1 (CP037909) from manure. A total of three IncFII type plasmids were discovered from these 18 plasmids and one of them is a subtype (IncFII[pCRY]) of IncFII plasmid type. IncFII(pCRY) type plasmid pSDP9R-*tetX4* which was collected from *K. pneumoniae* SDP9R showed high similarity with *tet(X4)*-negative plasmid pKP18-3-8-IncFII (MT035876) from human urine by BLASTn. Besides, three kinds of hybrid plasmids (IncFIA-IncHI1B-IncX1-IncN; IncFIA-IncHI1B-IncHIA; IncFIA-IncHI1B-IncX1) were also discovered. The hybrid plasmids showed high plasmid backbones similarities (BLASTN) with *tet(X4)*-positive plasmids pG3X16-2-3 (CP038140), pYSP8-1 (CP037911), pRF10-1_119k_*tetX* (MT219823), respectively.

Phylogenetic analysis. To further investigate the evolutionary relationship of 53 *E. coli* isolated from pork samples in this study and other *tet(X4)*-positive *E. coli* collected from human, pig farms and porcine slaughterhouses, a phylogenetic tree was constructed. The phylogenetic tree displayed that the *E. coli* strains were mainly grouped into four clusters (Fig. 3, S3). Among the 53 *E. coli*, the most abundant phylogenetic Clermont groups were groups A (29/53, 54.72%) and B1 (21/53 39.62%), whereas groups E (5.66%) was rare (Table S6). Besides, due to the blast comparison analysis found that pCSDP9R had high similarity with the *tet(X4)*-negative plasmids in *K. pneumoniae* isolated from clinical and environmental conditions (Fig. S4). So, a phylogenetic tree was constructed to analyze the genetic relationship between *K. pneumoniae* isolated from clinical or environmental, and the results showed that they are far related (Fig. S5).

According to the results of *tet(X4)*-positive strains MLST types, there were 26 distinct sequence types (STs) for *E. coli*, two ST types for *K. pneumoniae*, one ST type for *C. braakii*, one ST type for *C. freundii*, and one ST type for *K. quasipneumoniae*. The STs of *E. coli* were more diverse, with four main types (Fig. 4A), ST10 (8/53, 15.09%), ST48 (4/53, 7.5%), ST195 (4/53, 7.5%) and ST877 (5/53, 9.43%). Besides, same Inc type *tet(X4)*-positive plasmids could be identified not only from *E. coli* of the same ST types but also from the different ST types, which indicated the *tet(X4)* gene may spread between different ST type *E. coli* by plasmid horizontal transfer (Fig. 4B).

Transmissibility of *tet(X4)*-positive plasmids. Plasmids that carried *tet(X4)* from 22 strains were successfully transferred to *E. coli* C600. Besides, the conjugation frequency range of transconjugants was ranged from 10^{-6} to 10^{-3} , with most conjugal frequencies being 10^{-5} (Table S7). The conjugation frequency of IncX1 type plasmids was among 10^{-5} - 10^{-3} , which contains the highest conjugation frequency compared to other plasmid replication types in this study and was more likely to transfer.

The plasmids of four transconjugants were larger than the plasmids of their donor strains, except for one transconjugant plasmid pCAB12-1-*tetX4* which was smaller. Compared with the donor plasmid pAB12-1-*tetX4*, pCAB12-1-*tetX4* becomes smaller since some of the *tet(X4)* copy regions of pAB12-1-*tetX4* were lost during the transfer. Opposite to this, the reason that pCHS10-1-*tetX4* and pCSC4R-*tetX4* become bigger were mainly the increasing of copies of the *tet(X4)* region in the transconjugants.

Notably, two transconjugants CSZ11R and CSX5G showed much bigger than plasmids of the parental strain (Table S8), which mean the plasmid homologous recombination may

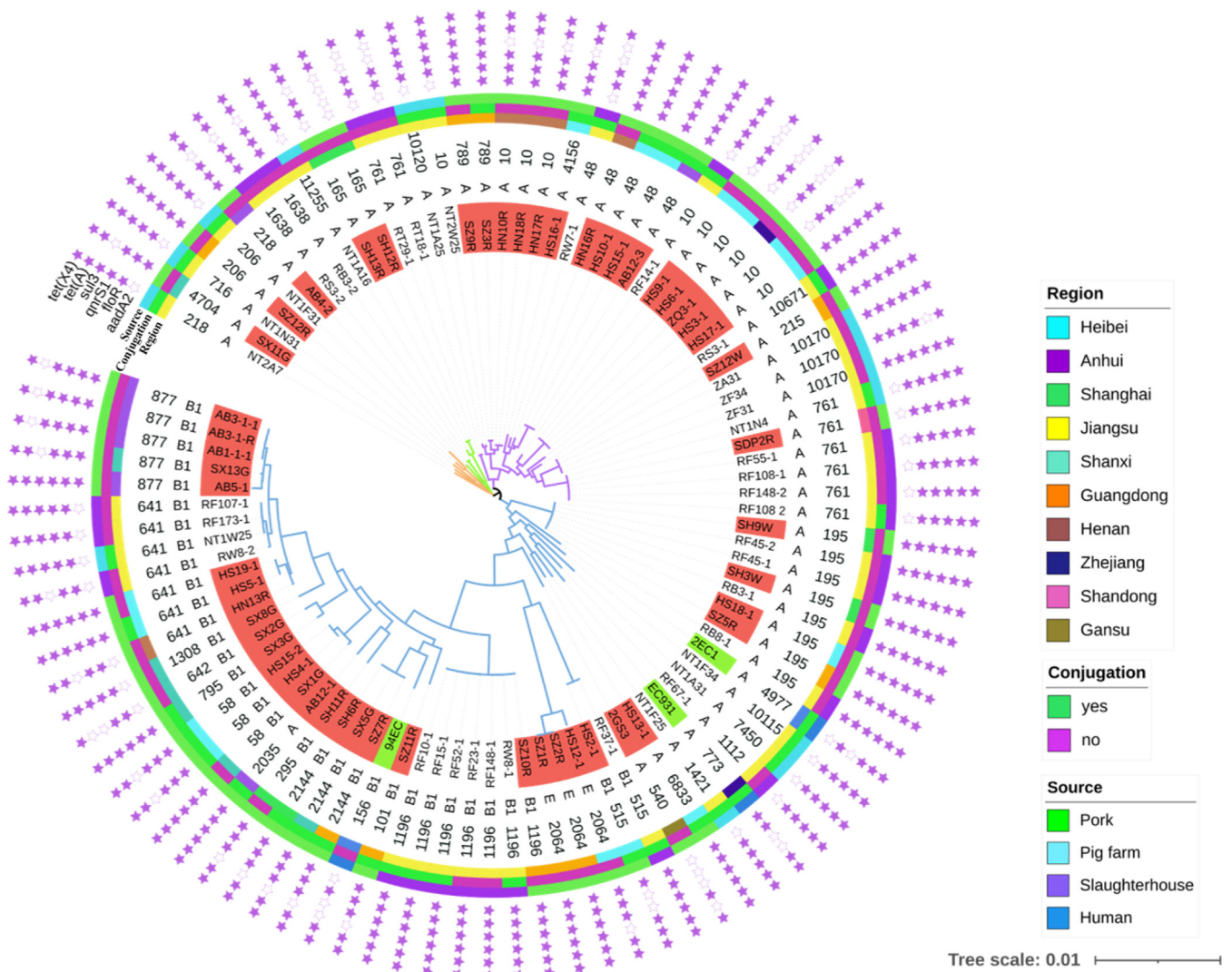


FIG 3 Phylogenetic tree of 96 *tet(X4)*-positive *E. coli* isolates from pork, human, pig farm and slaughterhouse. A total of four clusters (orange, green, purple and blue) were identified. The strains highlighted in red are from this study, green are from a human source. Resistance genes are indicated by asterisks, solid graphics indicate yes, hollow no.

occur (14–16). Detailed sequence analysis showed that 170 kb plasmid pSZ11R-170k and 56 kb plasmid pSZ11R-*tetX4* of parental strain formed a 256 kb size fusion plasmid pCSZ11R during the conjugation. Further intensive analyses revealed that two more 13 937 bp repeat segments *hp-tetR-tet(A)-lysR-floR-virD2-ISCR2-tet(X4)-abh-IS26-lnu(F)-aadA2-hp-IS26-ISPa40* were found in pCSZ11R compared with plasmids in SZ11R. The plasmid fusion mechanism are as follows, the insertion sequence IS26 located in plasmid pSZ11R-*tetX4* attacked the 10 bp size hot spot (GCTGTTCCAA) of pSZ11R-170k through intermolecular replicative transposition and resulted in IS26 repetition (Fig. 5A). This plasmid fusion mechanism resulted in 10 bp site sequence duplication and IS26 duplication. The 180 kb fusion plasmid pCSX5G-*tetX4* was formed by 122 kb size plasmid pSX5G-122k and 57 kb size plasmid pSX5G-*tetX4*, which has a similar fusion mechanism with pCSZ11R. The insertion sequence IS26 located in plasmid pSX5G-122k attacked the 5 bp size hot spot (TATCC) of pSX5G-*tetX4* through intermolecular replicative transposition and resulted in IS26 repetition (Fig. 5B).

The diversity of *tet(X4)*-harboring contexts and tandem repeats. The genetic environments of *tet(X4)* can be categorized into four groups (Fig. 6). The G1 ($n = 2$) can be classified as group 1, compared with the structure *ISCR2-ORF2-abh-tet(X4)-ISCR2* of original *tet(X4)*-carried plasmid p47EC (MK134376), G1 absent the *tet(X4)* downstream region

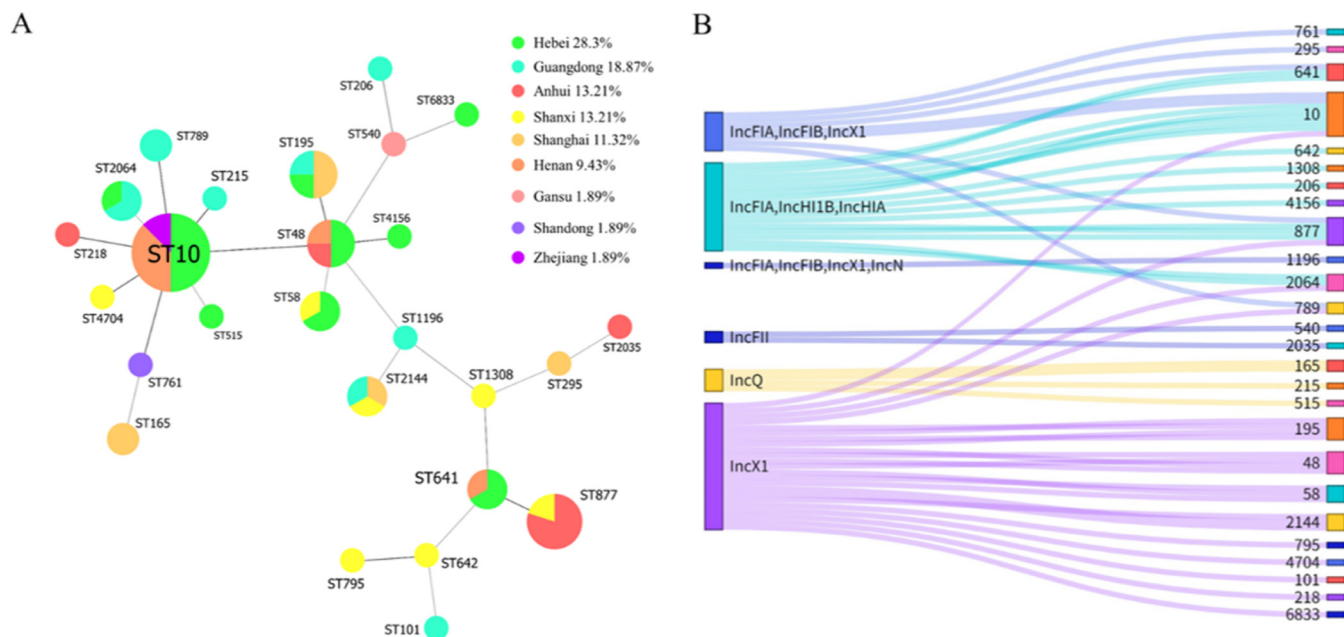


FIG 4 Phylogenetic trees of *E. coli* MLST and Sankey diagram. (A) Core genome MLST allelic profiles of *E. coli*. Guangdong and Hebei provinces with the most kinds of ST type. (B) Sankey diagram demonstrating the *tet(X4)*-positive *E. coli* ST types and the plasmid *Inc* type. The diameter of the line is proportional to the number of isolates, which is also labeled at the consolidation points.

ISCR2. Analyzed of group 2 (G2-2, $n = 1$; G2-3, $n = 1$), the *tet(X4)* upstream region of G2-2 is Δ *ISCR2* gene, which is the main difference between the *tet(X4)* genetic environment of p47EC. Group 3 (G3, $n = 22$; G3-1, $n = 12$; G3-2, $n = 2$; G3-3, $n = 1$) had the conserved structure *abh-tet(X4)-ISCR2-virD2-floR*, the difference between them is the upstream region with different gene (*ISCR2*, Δ *ISCR2*, *IS26*). The last group G4 (G4, $n = 16$; G4-1, $n = 1$) had two longest genetic region, *abh-tet(X4)-ISCR2-yheS-cat-zitR-ISCR2-virD2-floR* and *abh-tet(X4)-ISCR2-erm(26)-orf-orf-ISCR2-virD2-floR*. All four *tet(X4)* genetic environments were further analyzed by combined with the transmissibility, *E. coli* Phylogenetic group and the MIC of tigecycline (Fig. 7). The result displayed various and complex genetic environments of *tet(X4)*-positive *E. coli* during the *tet(X4)* gene spreading.

A total of five types repeat regions were discovered (Fig. S6), two repeat regions were detected in original plasmids (pHN13R-*tetX4*, 4 copy; pAB12-1-*tetX4*, multiple copy), and the others 3 kinds (pCSZ11R, 3 copy; pCHS10-1, 2 copy; pCSC4R, 4 copy) were found in transconjugants (pCSZ11R: *ISPA40-tetR-tet(A)-lysR-floR-virD2-ISCR2-tet(X4)-abh-IS26-lnu(F)-aadA2-IS26* 13,879 bp; pCHS10-1: *tet(X4)-abh-IS26-lnu(F)-aadA2-Int1-IS26* 7,445 bp; pCSC4R: *tet(X4)-abh-ISCR2-orf-ISCR2* 6,926 bp).

Fitness cost and plasmid stability. It is interesting to note that all three transconjugants contained a single plasmid showed equivalent growth rates to C600 (P value > 0.5) (Fig. S7A). Meanwhile, to compare the biofilm-forming abilities of *tet(X4)*-harboring transconjugants of different plasmid replicon types, we performed a biofilm assay. As shown in Fig. S7B, the transconjugant with pCSDP9R, pCAB12-1 or pCSC4R showed no difference in biofilm formation from the plasmid-free recipient strain C600.

In order to evaluate the stability of *tet(X4)* gene and *tet(X4)*-positive plasmids of different plasmid replicon types in the strains and their transconjugants, samples from the 10th, 20th, and 30th generations were selected for analysis. Under the pressure of tigecycline, the *tet(X4)* gene and *tet(X4)*-positive plasmid were inherited stably during the passage of strains (SC4R, SDP9R, AB12-1) and transconjugants (CSC4R, CSDP9R, CAB12-1). According to Fig. S8, *tet(X4)* was found in all 10th generation strains and transconjugants, clones negative for *tet(X4)* were detected in the 20th and 30th generation strains and transconjugants in the absence of tigecycline exposure. Most of the *tet(X4)* gene loss resulted from the loss of the plasmid carrying the *tet(X4)* gene. Loss

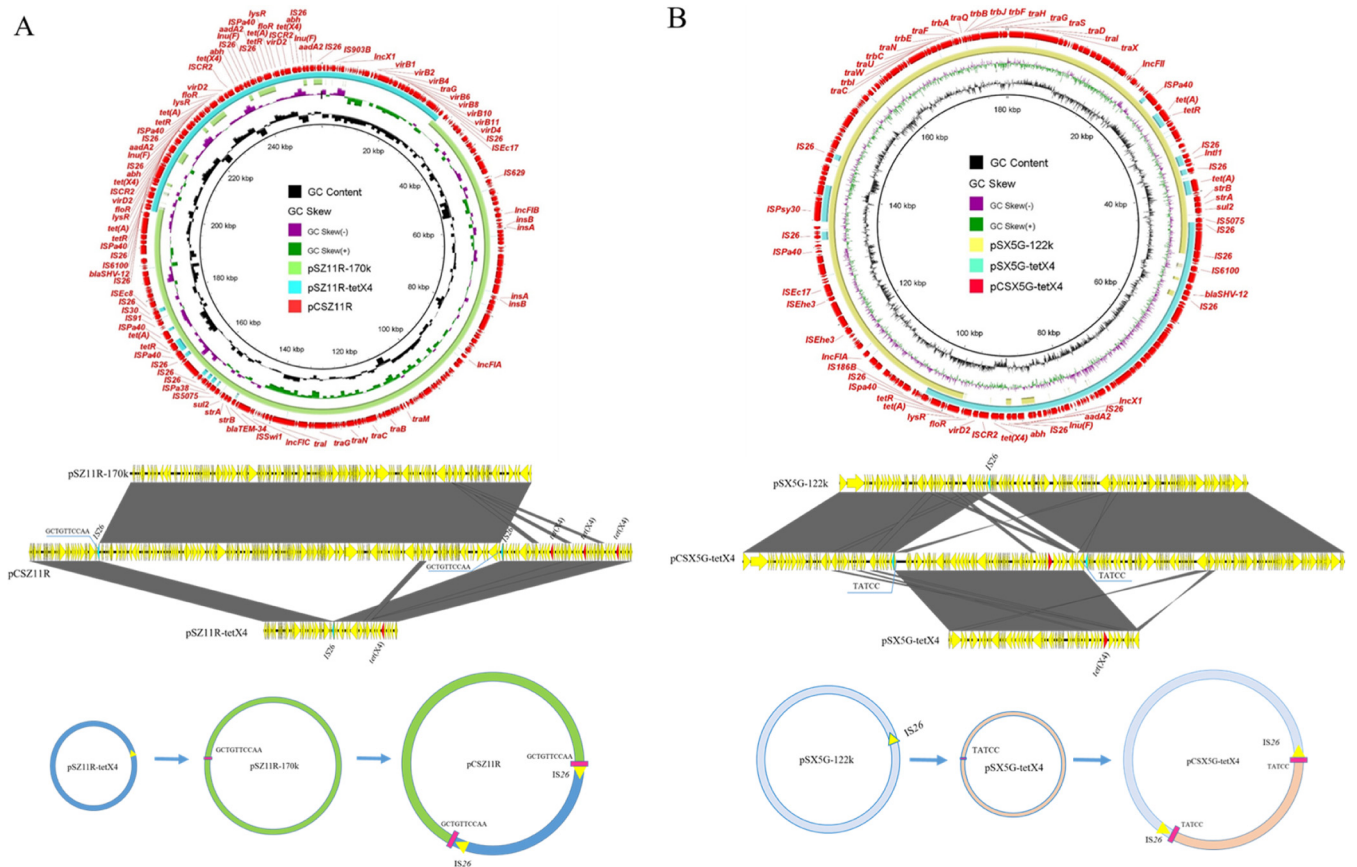


FIG 5 Mechanisms of fusion plasmids generation. (A) Formation mechanism of the fusion plasmid pCSZ11R. (B) Formation mechanism of the fusion plasmid pCSX5G-tetX4. The upper part denotes circular plasmid comparison between *tet(X4)*-positive plasmids in the transconjugants and their progenitor plasmids in the donor strains. The middle part denotes linear plasmid comparison between *tet(X4)*-positive plasmids and their progenitor plasmids, and the gray regions indicate the homologous region. At the bottom, proposed generation processes of two cointegrate plasmids were mediated by IS26.

of the *tet(X4)* gene in both strains SDP9R and CSDP9R resulted from a loss of the *tet(X4)*-positive plasmid.

To further explore the mechanism of *tet(X4)* loss but plasmid presence, plasmids of the single clone were picked out for Nanopore sequencing. Results are shown in Fig. S9, the comparison between the plasmids pAB12-1-*tetX4* and pAB12-1- Δ *tetX4* showed that the 77 kb region, including three 12 kb same regions *ISCR2-tet(X4)-abh-dgkA-ISCR2-lysR-floR-virD2-ISCR2* and three 8 kb same regions Δ *ISCR2-erm(26)-ISCR2-tet(X4)-abh-dgkA-\Delta**ISCR2* was lost in pAB12-1- Δ *tetX4*. Detailed analysis of the transconjugants pCAB12-1 and pCAB12-1- Δ *tetX4* showed that pCAB12-1- Δ *tetX4* lost the 24 kb region compared with pCAB12-1, which contained multiple resistance genes such as *sul2*, *floR* and *tet(X4)* gene. Besides, compared with pSC4R-*tetX4*, the plasmid pSC4R- Δ *tetX4* lost the 27 kb region, including four 7 kb same regions *ISCR2-tet(X4)-abh-\Delta**ISCR2*. And the comparison between the transconjugants plasmids pCSC4R and pCSC4R- Δ *tetX4* indicated that the 7 kb region was lost in pCSC4R- Δ *tetX4*.

Copy numbers change. To further analyze the relationship between *ISCR2* and *tet(X4)*, the contact of copy number between *ISCR2* and *tet(X4)* was analyzed by Illumina sequencing data. We found that 49 (84.48%) of 58 *tet(X4)*-positive strains contained one copy of *tet(X4)*, and 9 (15.52%) of 58 possessed two or more copies of *tet(X4)*. And the copy number of *ISCR2* was always greater than or equal to the number of *tet(X4)* in the strain (Fig. S10). Besides, the copy number change of *tet(X4)* and *ISCR2* gene in CSZ11R and 30th passaged strains was also analyzed by Nanopore sequencing raw reads. The number of *tet(X4)* and *ISCR2* genes in 30th passaged strains were all increased compared with CSZ11R. More interestingly, the copy number of *ISCR2* on the same contig is always more than or equal to the *tet(X4)* gene.

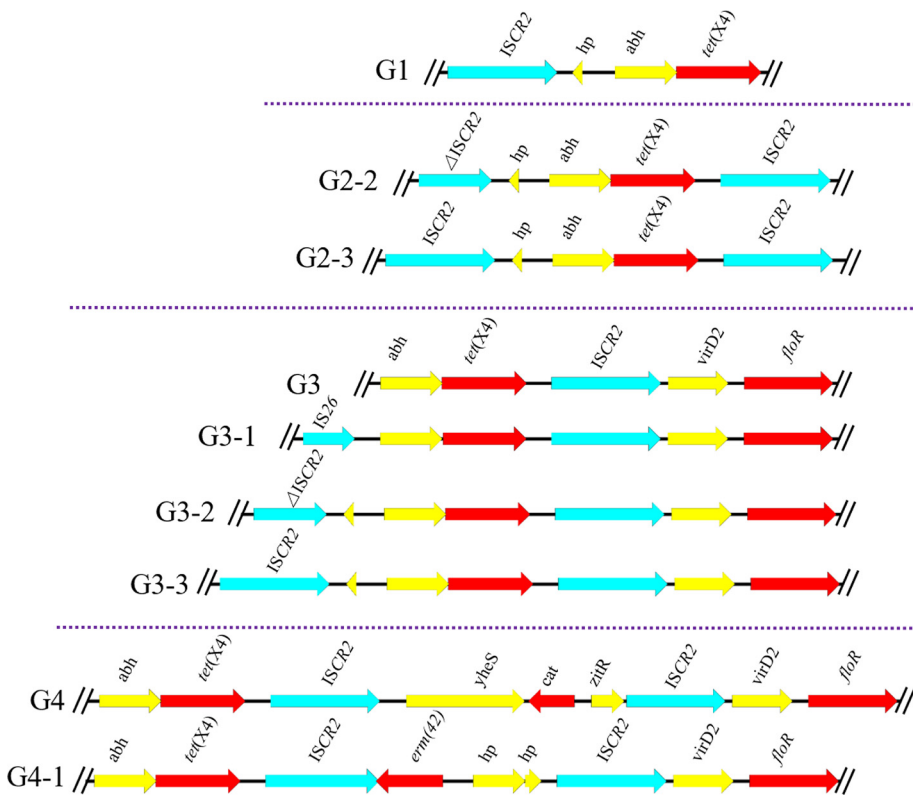


FIG 6 Different types of genetic environments of *tet(X4)* genes. Major types of *tet(X4)*-bearing genetic contexts among the 58 *tet(X4)*-bearing plasmids.

To explore the absolute expression of *tet(X4)* in different strains that contain different numbers *tet(X4)*, high linearity ($R^2 \geq 0.997$) standard curves were recovered by qRT-PCR assay (Fig. S11A). Expression levels of *tet(X4)* gene between different strains which contained different number *tet(X4)* gene was approximate (Table S9). Notably, the expression of *tet(X4)* gene in these strains with 4 mg/liter tigecycline was increased slightly than that without strains. Besides, the relative expression of *tet(X4)* gene (Fig. S11B) according to the result of relative quantification, rising with the concentration of tigecycline.

DISCUSSION

In this study, we isolated *tet(X4)*-bearing strains in pork samples from various areas in China and conducted a comprehensive molecular typing study. A multitude of different *tet(X4)*-positive strains have been isolated from pork samples. Although the *tet(X4)*-positive *E. coli* have been reported in several articles (17–19), to the best of our knowledge, this is the first study that *tet(X4)* gene has been identified in *K. pneumoniae*, *K. quasipneumoniae*, *C. braakii*, and *C. freundii* from pork samples. Besides, the *tet(X4)*-positive plasmids in this study were mainly found in *E. coli*, indicated that *E. coli* is a huge reservoir of *tet(X4)*-positive plasmids. All the *tet(X4)*-carrying strains exhibited high resistance to tigecycline (8 mg/liter-64 mg/liter), and they also confer resistance to multiple classes of antibiotics, which could bring great difficulty to the clinic treatment.

Several reports indicate that IS26 could mediate the fusion of other plasmids to form MDR plasmids (20, 21). This suggested that IS26 played an important role in the transfer of *tet(X4)* and may promote the evolution of the *tet(X4)*-positive plasmids. The plasmids size changes due to the *tet(X4)* copy number variation during the transfer experiments, imply the number of *tet(X4)* may not stable during the conjugation assay.

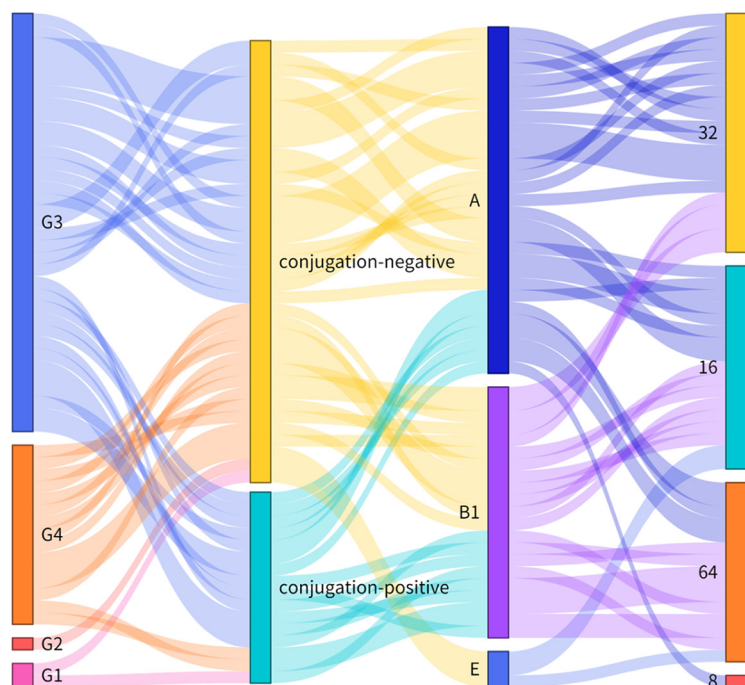


FIG 7 Sankey diagram combining the genetic environments bearing *tet(X4)*, conjugation, *E. coli* group and the MIC for tigecycline. The diameter of the line is proportional to the number of isolates, which is also labeled at the consolidation points.

Furthermore, the tandem repeated regions of *tet(X4)* were also found in two parental strains that were different from the previous article (8, 13, 22, 23). Unlike the tandem duplication of other genes (24), the MICs of *tet(X4)* tandem repeat strains to tigecycline were not increased significantly, which is a strange phenomenon that needs us to further investigations.

The phylogenetic tree displayed *E. coli* strains from pork samples, human source samples, pig farms and porcine slaughterhouses are not in independent clade, which implies that *tet(X4)*-positive *E. coli* may spread along the entire production chain and pose a great threat to human health care and animal food production. Despite the ST type of *tet(X4)*-positive *E. coli* isolated from human source is different from other *tet(X4)*-positive *E. coli* in this study, the IncX1 type plasmid carrying the *tet(X4)* gene in strain EC931 that isolated from human has a high similarity with the same Inc type plasmid carrying the *tet(X4)* gene in this study. Besides, the *tet(X4)* gene from strain 2EC1 that collected from human source was located on a conjugative plasmid. This phenomenon indicated that *tet(X4)* in human and pig sources may have the risk of mutual transmission through plasmids. It has been proved in previous literature that the phylogroups A and B1 could exhibit an increased drug resistance pattern (25). Besides, the phylogenetic groups of *tet(X4)*-positive *E. coli* in pork, pig farms and pig slaughterhouses were mainly group A, followed by group B1. It has previously been shown that *E. coli* isolated from human feces is mainly group A, while it is mainly group B1 in animals (27, 28). In this study, *E. coli* belonged to group A carrying multiple drug resistance genes may be more likely to infect staff involved in the pig production chain. Moreover, the diversity of MLST types showed that the *tet(X4)*-carrying *E. coli* strains isolated from pork, pig farm and slaughterhouse were diverse, indicating that plasmids may play an important role in the spread of *tet(X4)* genes among *E. coli*.

Unlike other tandem repeat resistance genes (24, 29), the increased copy number of *tet(X4)* did not enhance the resistance of the strains to tigecycline (13, 30). The expression of *tet(X4)* carried by different *tet(X4)* copy number strains showed no significant difference according to the result of absolute quantitative, which illustrated that the

sensitivity of strains to tigecycline with different *tet(X4)* copy number has no change and the contribution from *tet(X4)* amplification can be omitted. The increase in *tet(X4)* copy number with increased tigecycline concentration, which illustrated that the expression of the *tet(X4)* gene could increase under the pressure of the tigecycline drug. Insertion sequence *ISCR2* belongs to *ISCR* elements and shares 65% amino acid identity with *ISCR1* (31). Until now, *ISCR2* has been found adjacent to multiple resistant genes such as *floR*, *tetA*, *tetR*, *strA*, *strB*, *tet(X4)* and *sul2* collected in multiple plasmids from different sources (13, 32). More interestingly, the copy number of *ISCR2* has always increased together with the *tet(X4)* gene. Several published reports have indicated *ISCR2* which is surrounded by *tet(X4)* could form a circular intermediate and may transfer to other plasmids and chromosomes. This circular intermediate may recognize an *ISCR2* site and then insertion there produced a new copy, thus lead to a tandem repeat of the *tet(X4)* gene.

Despite the findings, this work has several limitations. First, we only focused on the tigecycline-resistant strains by utilizing selective recovery strategy with agar plates supplemented with tigecycline. Thus, the prevalence of isolation of tigecycline resistance in each bacterial species was not available, which is a limit of this study. Second, a low number of pork samples and sampling bias may affect the positive rates observed in different regions.

In conclusion, this study conducted an in-depth analysis of pork samples from multi-region across the country, expanding our understanding of the diversity and complexity of *tet(X4)*-positive plasmids in pork. The *tet(X4)* gene was found carried by a variety of Gram-negative bacteria and different plasmid types, which greatly increase the risk of *tet(X4)* transmission. Multiple and complex *tet(X4)* genetic environments expands their host range and poses a serious threat to human health and food safety. The insertion sequences *IS26* and *ISCR2* play an important role in plasmid fusion and drug resistance genes transfer, which suggested more attention should be paid to the role of these mobile genetic elements. Besides, effective and reasonable measures should be formulated to ensure the safety of the pork production chain.

MATERIALS AND METHODS

Bacterial isolates. The fresh pork samples were randomly collected from local supermarkets and retail stores across nine provinces (Shanxi, Shandong, Sichuan, Guangdong, Gansu, Henan, Anhui, Hebei, Zhejiang) and one municipality (Shanghai) of China. Tigecycline resistant Enterobacteriaceae were selected on MacConkey agar plates containing tigecycline (4 mg/liter). Bacterial species identifications of purified strains were performed using the 16S rRNA gene sequencing. The *tet(X4)* resistance gene was determined by PCR with reported primers (8).

Antimicrobial susceptibility testing. The MICs of *tet(X4)*-positive strains against 13 antibiotics were conducted by broth microdilution using 96-well plates. *E. coli* ATCC 25922 was used as the quality control strain. Resistance breakpoint was interpreted according to the EUCAST criteria (>2 mg/liter) for tigecycline and CLSI guidelines (33) for the remaining antibiotics.

Conjugation experiments. Transferability of *tet(X4)* was determined by filter mating conjugation experiments using *tet(X4)*-positive strains as the donor strains and rifampicin-resistant *E. coli* C600 (Rif^r) as the recipient (1:4) at 37°C. The transconjugants were recovered on LB agar plates containing tigecycline (4 mg/liter) together with rifampin (300 mg/liter). PCR and S1-PFGE were used to further confirm the transconjugants. Transfer frequencies were calculated as the number of transconjugants/total number of recipients.

Whole-genome sequencing. The genomes of tigecycline resistant strains were extracted with the TIANamp Genomic DNA kit (TianGen, Beijing, China) and quantified by Qubit 4 Fluorometer. Then the genomic DNA samples were sequenced using Illumina HiSeq 2500 platform. The paired-end reads were *de novo* assembled using SPAdes version 3.14.0. According to phylogenetic analysis and resistant phenotypes, 18 representative isolates were selected for further sequencing by long-read Nanopore sequencing. Complete genome sequences were obtained using Unicycler version 0.4.8 with the default parameters (34). For MDR regions that could not be resolved by short-read data or even hybrid assembly method, long reads assembly tool Flye version 2.4.2 was used to confirm the accurate structures of complex MDR regions in genomes (35).

Bioinformatics analysis. The assembled sequences were annotated through RAST online server (<https://rast.nmpdr.org/>) automatically. ResFinder, PlasmidFinder and ISfinder were used to detect the antibiotic resistance genes (ARGs), plasmid replicon types and insertion sequences (36–38). For each *tet(X4)* carrying strain that was only sequenced with the second-generation sequencing technique, the contigs acquired by Illumina sequencing of them were aligned with *tet(X4)*-positive circular plasmids carrying different replicons to obtain the *tet(X4)*-positive plasmid types (39). Virulence genes were

determined using the ABRicate (<https://github.com/tseemann/abricate>) and Kleborate (<https://github.com/katholt/Kleborate>). BRIG and Easyfig were used to display plasmid comparison maps (40, 41). Multilocus sequence type (MLST) of all *tet(X4)*-positive isolates were assigned using the mlst tool (<https://github.com/tseemann/mlst>). The core genome MLST allelic profiles of *E. coli* was built using PHYLOVIZ (42). The phylotyping of *E. coli* was performed using clermont.py software (<https://github.com/A-BN/ClermonTyping>). Phylogenetic trees of *E. coli* and *K. pneumoniae* were constructed using Roary and FastTree based on single nucleotide polymorphisms (SNPs) of core genomes (26, 43). The resulting phylogeny was visualized and retouched using iTol (<https://itol.embl.de>).

Fitness cost of *tet(X4)*-positive plasmids. To investigate the fitness cost of *tet(X4)*-positive plasmids, growth curves for the *E. coli* strain C600 and transconjugants with different *tet(X4)*-positive plasmids were performed in 96-well flat-bottom plates. *E. coli* strain C600 and different transconjugants bearing diverse *tet(X4)*-positive plasmids were inoculated in a test tube containing 5 ml of LB broth, and shaken cultures at a constant temperature, 37°C for 24 h. 200 μ l of each culture were then added in triplicate to 96-well flat-bottom plates every 1 h to test OD600 and continue to culture the remaining bacteria. Growth curves were plotted using GraphPad Prism software.

Biofilm formation. The *E. coli* strain C600 and three transconjugants with diverse *tet(X4)*-positive plasmids were inoculated into 10 ml test tubes containing 5 ml of LB broth and then incubated overnight at 37°C. 200 μ l of each culture were then added in triplicate to 96-well flat-bottom plates and incubated at 37°C for 24 h. The cells were washed twice with phosphate-buffered saline (PBS) and stained with 0.1% crystal violet for 20 min at room temperature. The wells were dried, and the bound dye was solubilized with 100 μ l of 33% acetic acid for 30 min. Absorbance values were quantified by measuring the absorbance at 570 nm. A well containing sterile LB without bacteria served as the negative control. Each experiment was performed in duplicate and repeated three times.

Plasmid stability and evolution of *tet(X4)* duplications. Strains and corresponding transconjugants of different plasmid replicon types were grown on LB agar overnight, then single clones were randomly selected to passage for 15 days in LB broth medium with or without antibiotic pressure. 96 single clones of 10th, 20th and 30th passages were picked out separately, and the presence of *tet(X4)* and plasmid replicon was validated by PCR. To explore the copy numbers changes in passaged strains, strain CSC4R was tested under the pressure with tigecycline. Single clones were picked out from 30th generation bacteria with tigecycline. The MIC values of strains to tigecycline were tested by broth microdilution and Nanopore sequencing was used to visualize changes in *tet(X4)* copy number.

Detection of copy numbers and expressions of *tet(X4)* by real-time PCR. The qPCR target genes were amplified using the following forward and reverse primers: 16s-*E. coli* F: CCTACGGGAGGCAGCAG and R: ATTACCGCGTCTGCTGG *TetX4* F: ATAATTGGTGGTGACCCGT and R: AATTCTTGCCTCTCGTCTCGT. Plasmid pCE2 containing *tet(X4)* was used to generate standard curves. Strains (SZ11R, CSZ11R, CSC4R) contained different *tet(X4)* numbers were used as samples and incubated with or without tigecycline (4 mg/liter). The copy numbers of plasmid DNA per microliter were calculated using the following formula, copies of 1 μ l = $6.02 \times 10^{23} \times \text{DNA mass concentration (ng}/\mu\text{l}) \times 10^{-9}/(\text{plasmid vector size} + \text{amplicon size bp}) * 660$. Besides, the relative expression of *tet(X4)* was also measured, with the gene 16s-*E. coli* serving as the internal control. Different concentrations of tigecycline were used to act on *tet(X4)* gene single-copy strain DH5 α , which was constructed by chemical transformation. Each reaction was run in triplicate.

Data availability. The sequences obtained in this paper have been deposited in the GenBank database under BioProject number PRJNA665928. The sequences of transconjugants with only Nanopore data analyzed individually were deposited in the figshare database (<https://figshare.com/s/fce84af26b4ee188503d>) for reference.

SUPPLEMENTAL MATERIAL

Supplemental material is available online only.

SUPPLEMENTAL FILE 1, PDF file, 2.1 MB.

ACKNOWLEDGMENTS

This work was supported by the National Natural Science Foundation of China (no. 31872523 and 31872526), Jiangsu Agriculture Science and Technology Innovation Fund (JASTIF, no. CX[21]3138), the China Postdoctoral Science Foundation (no. 2020M671632) and the Priority Academic Program Development of Jiangsu Higher Education Institutions (PAPD).

REFERENCES

- Laxminarayan R, Sridhar D, Blaser M, Wang MG, Woolhouse M. 2016. Achieving global targets for antimicrobial resistance. *Science* 353: 874–875. <https://doi.org/10.1126/science.aaf9286>.
- Karageorgopoulos DE, Falagas ME. 2008. Current control and treatment of multidrug-resistant *Acinetobacter baumannii* infections. *Lancet Infectious Diseases* 8:751–762. [https://doi.org/10.1016/S1473-3099\(08\)70279-2](https://doi.org/10.1016/S1473-3099(08)70279-2).
- Markley JL, Wenczewicz TA. 2018. Tetracycline-Inactivating Enzymes. *Front Microbiol* 9:1058. <https://doi.org/10.3389/fmicb.2018.01058>.
- Chopra I, Roberts M. 2001. Tetracycline antibiotics: mode of action, applications, molecular biology, and epidemiology of bacterial resistance. *Microbiol Mol Biol Rev* 65:232–260. <https://doi.org/10.1128/MMBR.65.2.232-260.2001>.

5. Sun Y, Cai Y, Liu X, Bai N, Liang B, Wang R. 2013. The emergence of clinical resistance to tigecycline. *Int J Antimicrob Agents* 41:110–116. <https://doi.org/10.1016/j.ijantimicag.2012.09.005>.
6. Deng M, Zhu MH, Li JJ, Bi S, Sheng ZK, Hu FS, Zhang JJ, Chen W, Xue XW, Sheng JF, Li LJ. 2014. Molecular epidemiology and mechanisms of tigecycline resistance in clinical isolates of *Acinetobacter baumannii* from a Chinese university hospital. *Antimicrob Agents Chemother* 58:297–303. <https://doi.org/10.1128/AAC.01727-13>.
7. Du PC, Zhang YY, Chen C. 2018. Emergence of carbapenem-resistant hypervirulent *Klebsiella pneumoniae*. *Lancet Infectious Diseases* 18:23–24. [https://doi.org/10.1016/S1473-3099\(17\)30625-4](https://doi.org/10.1016/S1473-3099(17)30625-4).
8. He T, Wang R, Liu DJ, Walsh TR, Zhang R, Lv Y, Ke YB, Ji QJ, Wei RC, Liu ZH, Shen YB, Wang G, Sun LC, Lei L, Lv ZQ, Li Y, Pang MD, Wang LY, Sun QL, Fu YL, Song HW, Hao YX, Shen ZQ, Wang SL, Chen GX, Wu CM, Shen JZ, Wang Y. 2019. Emergence of plasmid-mediated high-level tigecycline resistance genes in animals and humans. *Nat Microbiol* 4:1450–1456. <https://doi.org/10.1038/s41564-019-0445-2>.
9. He T, Wei R, Li R, Zhang L, Sun L, Bao H, Gu J, Wang Y, Wang R. 2020. Co-existence of tet(X4) and mcr-1 in two porcine *Escherichia coli* isolates. *J Antimicrob Chemother* 75:764–766. <https://doi.org/10.1093/jac/dkz510>.
10. Li Y, Wang Q, Peng K, Liu Y, Li R, Wang Z. 2020. Emergence of Carbapenem- and Tigecycline-Resistant *Proteus cibarius* of Animal Origin. *Front Microbiol* 11:1940. <https://doi.org/10.3389/fmicb.2020.01940>.
11. Chen C, Chen L, Zhang Y, Cui CY, Wu XT, He YZ, Cui ZH, Li C, Jia QL, Shen XG, Sun RY, Wang XR, Wang MG, Tang T, Zhang Y, Liao XP, Kreiswirth BN, Zhou SD, Huang B, Du H, Sun J, Chen L, Liu YH. 2020. Genetic diversity and characteristics of high-level tigecycline resistance Tet(X) in *Acinetobacter* species. *Genome Med* 12:111. <https://doi.org/10.1186/s13073-020-00807-5>.
12. Li R, Lu X, Peng K, Liu Z, Li Y, Liu Y, Xiao X, Wang Z. 2020. Deciphering the structural diversity and classification of the mobile tigecycline resistance gene tet(X)-bearing plasmidome among bacteria. *mSystems* 5. <https://doi.org/10.1128/mSystems.00134-20>.
13. He DD, Zhu YY, Li RC, Pan YS, Liu JH, Yuan L, Hu GZ. 2019. Emergence of a hybrid plasmid derived from IncN1-F33A-B- and mcr-1-bearing plasmids mediated by IS26. *J Antimicrob Chemother* 74:3184–3189. <https://doi.org/10.1093/jac/dkz327>.
14. Liu ZY, Xiao X, Liu Y, Li RC, Wang ZQ. 2020. Recombination of NDM-5-producing plasmids mediated by IS26 among *Escherichia coli*. *Int J Antimicrob Agents* 55:105815. <https://doi.org/10.1016/j.ijantimicag.2019.09.019>.
15. Li RC, Lu XY, Peng K, Liu Y, Xiao X, Wang ZQ. 2020. Reorganization of mcr-1-bearing large MDR plasmids resolved by nanopore sequencing. *J Antimicrob Chemother* 75:1645–1647. <https://doi.org/10.1093/jac/dkaa046>.
16. Sun J, Chen C, Cui CY, Zhang Y, Liu X, Cui ZH, Ma XY, Feng YJ, Fang LX, Jian XL, Zhang RM, Tang YZ, Zhang KX, Liu HM, Zhuang ZH, Zhou SD, Lv LN, Du H, Huang B, Yu FY, Mathema B, Kreiswirth BN, Liao XP, Chen L, Liu YH. 2019. Plasmid-encoded tet(X) genes that confer high-level tigecycline resistance in *Escherichia coli*. *Nat Microbiol* 4:1457–1464. <https://doi.org/10.1038/s41564-019-0496-4>.
17. Bai L, Du P, Du Y, Sun H, Zhang P, Wan Y, Lin Q, Fanning S, Cui S, Wu Y. 2019. Detection of plasmid-mediated tigecycline-resistant gene tet(X4) in *Escherichia coli* from pork, Sichuan and Shandong Provinces, China, February 2019. *Euro Surveill* 24. <https://doi.org/10.2807/1560-7917.ES.2019.24.25.1900340>.
18. Ding Y, Saw WY, Tan LWL, Moong DKN, Nagarajan N, Teo YY, Seedorf H. 2020. Emergence of tigecycline- and eravacycline-resistant tet(X4)-producing Enterobacteriaceae in the gut microbiota of healthy Singaporeans. *J Antimicrob Chemother* 75:3480–3484. <https://doi.org/10.1093/jac/dkaa372>.
19. He SS, Hickman AB, Varani AM, Siguier P, Chandler M, Dekker JP, Dyda F. 2015. Insertion sequence IS26 reorganizes plasmids in clinically isolated multidrug-resistant bacteria by replicative transposition. *mBio* 6. <https://doi.org/10.1128/mBio.00762-15>.
20. Du P, Liu D, Song H, Zhang P, Li R, Fu Y, Liu X, Jia J, Li X, Fanning S, Wang Y, Bai L, Zeng H. 2020. Novel IS26-mediated hybrid plasmid harbouring tet(X4) in *Escherichia coli*. *J Glob Antimicrob Resist* 21:162–168. <https://doi.org/10.1016/j.jgar.2020.03.018>.
21. Li R, Lu X, Liu Z, Liu Y, Xiao X, Wang Z. 2020. Rapid detection and characterization of tet(X4)-positive *Escherichia coli* strains with nanopore sequencing. *J Antimicrob Chemother* 75:1068–1070. <https://doi.org/10.1093/jac/dkz528>.
22. Song H, Liu D, Li R, Fu Y, Zhai W, Liu X, He T, Wu C, Bai L, Wang Y. 2020. Polymorphism existence of mobile tigecycline resistance gene tet(X4) in *Escherichia coli*. *Antimicrob Agents Chemother* 64. <https://doi.org/10.1128/AAC.01825-19>.
23. Sun L, Chen Y, Hua X, Chen Y, Hong J, Wu X, Jiang Y, van Schaik W, Qu T, Yu Y. 2019. Tandem amplification of the vanM gene cluster drives vancomycin resistance in vancomycin-variable enterococci. *J Antimicrob Chemother* 75:283–291. <https://doi.org/10.1093/jac/dkz461>.
24. Smith JL, Fratamico PM, Gunther NW. 2007. Extraintestinal pathogenic *Escherichia coli*. *Foodborne Pathog Dis* 4:134–163. <https://doi.org/10.1089/fpd.2007.0087>.
25. Page AJ, Cummins CA, Hunt M, Wong VK, Reuter S, Holden MT, Fookes M, Falush D, Keane JA, Parkhill J. 2015. Roary: rapid large-scale prokaryote pan genome analysis. *Bioinformatics* 31:3691–3693. <https://doi.org/10.1093/bioinformatics/btv421>.
26. Stoppe NC, Silva JS, Carlos C, Sato MIZ, Saraiva AM, Ottoboni LMM, Torres TT. 2017. Worldwide phylogenetic group patterns of *Escherichia coli* from commensal human and wastewater treatment plant isolates. *Front Microbiol* 8:2512. <https://doi.org/10.3389/fmicb.2017.02512>.
27. Carlos C, Pires MM, Stoppe NC, Hachich EM, Sato MI, Gomes TA, Amaral LA, Ottoboni LM. 2010. *Escherichia coli* phylogenetic group determination and its application in the identification of the major animal source of fecal contamination. *BMC Microbiol* 10:161. <https://doi.org/10.1186/1471-2180-10-161>.
28. Hubbard ATM, Mason J, Roberts P, Parry CM, Corless C, van Aartsen J, Howard A, Fraser AJ, Adams RB, Roberts AP, Edwards T. 2020. Within-patient evolution to piperacillin/tazobactam resistance in a clinical isolate of *Escherichia coli* due to IS26-mediated amplification of blaTEM-1B. <https://doi.org/10.1101/2020.02.28.969360>.
29. Li R, Lu X, Liu Z, Liu Y, Xiao X, Wang Z. 2020. Rapid detection and characterization of tet(X4)-positive *Escherichia coli* strains with nanopore sequencing. *J Antimicrob Chemother* 75:1068–1070. <https://doi.org/10.1093/jac/dkz528>.
30. Xu Y, Wang C, Zhang G, Tian J, Liu Y, Shen X, Feng J. 2017. ISCR2 is associated with the dissemination of multiple resistance genes among *Vibrio* spp. and *Pseudoaeromonas* spp. isolated from farmed fish. *Arch Microbiol* 199:891–896. <https://doi.org/10.1007/s00203-017-1365-2>.
31. Fernandez-Alarcon C, Singer RS, Johnson TJ. 2011. Comparative genomics of multidrug resistance-encoding IncA/C plasmids from commensal and pathogenic *Escherichia coli* from multiple animal sources. *PLoS One* 6: e23415. <https://doi.org/10.1371/journal.pone.0023415>.
32. Anonymous. 2018. Performance Standards for Antimicrobial Susceptibility Testing—Twenty-Seventh Informational Supplement: M100. CLSI.
33. Wick RR, Judd LM, Gorrie CL, Holt KE. 2017. Unicycler: resolving bacterial genome assemblies from short and long sequencing reads. *PLoS Comput Biol* 13:e1005595. <https://doi.org/10.1371/journal.pcbi.1005595>.
34. Kolmogorov M, Yuan J, Lin Y, Pevzner PA. 2019. Assembly of long, error-prone reads using repeat graphs. *Nat Biotechnol* 37:540–546. <https://doi.org/10.1038/s41587-019-0072-8>.
35. Carattoli A, Zankari E, Garcia-Fernandez A, Larsen MV, Lund O, Villa L, Aarestrup FM, Hasman H. 2014. In silico detection and typing of plasmids using plasmidfinder and plasmid multilocus sequence typing. *Antimicrob Agents Chemother* 58:3895–3903. <https://doi.org/10.1128/AAC.02412-14>.
36. Siguier P, Perochon J, Lestrade L, Mahillon J, Chandler M. 2006. ISfinder: the reference centre for bacterial insertion sequences. *Nucleic Acids Res* 34:D32–D36. <https://doi.org/10.1093/nar/gkj014>.
37. Bortolaia V, Kaas RS, Ruppe E, Roberts MC, Schwarz S, Cattoir V, Philippon A, Allesoe RL, Rebelo AR, Florensa AF, Fagelhauer L, Chakraborty T, Neumann B, Werner G, Bender JK, Stingl K, Nguyen M, Coppens J, Xavier BB, Malhotra-Kumar S, Westh H, Pinholt M, Anjum MF, Duggett NA, Kempf I, Nykasanen S, Olkkola S, Wiczorek K, Amaro A, Clemente L, Mossong J, Losch S, Ragimbeau C, Lund O, Aarestrup FM. 2020. ResFinder 4.0 for predictions of phenotypes from genotypes. *J Antimicrob Chemother* 75:3491–3500. <https://doi.org/10.1093/jac/dkaa345>.
38. Jiang Y, Zhang Y, Lu J, Wang Q, Cui Y, Wang Y, Quan J, Zhao D, Du X, Liu H, Li X, Wu X, Hua X, Feng Y, Yu Y. 2020. Clinical relevance and plasmid dynamics of mcr-1-positive *Escherichia coli* in China: a multicentre case-control and molecular epidemiological study. *Lancet Microbe* 1:e24–e33. [https://doi.org/10.1016/S2666-5247\(20\)30001-X](https://doi.org/10.1016/S2666-5247(20)30001-X).
39. Alikhan NF, Petty NK, Ben Zakour NL, Beatson SA. 2011. BLAST Ring Image Generator (BRIG): simple prokaryote genome comparisons. *BMC Genomics* 12:402. <https://doi.org/10.1186/1471-2164-12-402>.

41. Sullivan MJ, Petty NK, Beatson SA. 2011. Easyfig: a genome comparison visualizer. *Bioinformatics* 27:1009–1010. <https://doi.org/10.1093/bioinformatics/btr039>.
42. Ribeiro-Goncalves B, Francisco AP, Vaz C, Ramirez M, Carrico JA. 2016. PHYLOViZ Online: web-based tool for visualization, phylogenetic inference, analysis and sharing of minimum spanning trees. *Nucleic Acids Res* 44: W246–51. <https://doi.org/10.1093/nar/gkw359>.
43. Price MN, Dehal PS, Arkin AP. 2009. FastTree: computing large minimum evolution trees with profiles instead of a distance matrix. *Mol Biol Evol* 26: 1641–1650. <https://doi.org/10.1093/molbev/msp077>.